Optimum dimensions of plate fins for fin–tube heat exchangers

B. Kundu and P. K. Das
Department of Mechanical Engineering, Indian Institute of Technology, Kharagpur, India

Optimum dimensions of the fin for the fin–tube heat exchangers are determined in this study for both rectangular and equilateral triangular arrays of tubes. Maximum heat dissipation is obtained for a particular value of pitch length or fin thickness for a fixed fin volume. The optimization is done by the classical derivative method. Based on the mathematical analysis, design curves have been constructed for the design of optimum fins. Finally, it is verified that the concept of equivalent annular fin can be extended to calculate the optimum fin dimensions.

Keywords: equivalent annular fin; hexagonal fin; optimum fin thickness; plate fin heat exchanger; square fin

Introduction

Fin tube heat exchangers are employed for the exchange of heat between a gas and a liquid. These heat exchangers have extensive applications in refrigeration, HVAC systems, and as automobile radiators. Integral fin–tube geometry is also often selected as the design of dry coolers of power plants and process heat exchangers in the chemical industry. Poor heat transfer of the gas side is improved by attaching fins to the outer periphery of the liquid carrying tubes. Although certain designs employ individual circumferential fins for each of the tubes, in most applications, continuous fin sheets pierced by regular arrays of tubes are used. The latter arrangement is not only simple and economic, but also increases overall rigidity of the structure. The augmentation of heat transfer is associated with the increased volume, weight, and cost of the heat exchanger because of the addition of fins. However, tube spacing and fin thickness can be selected optimally so that maximum heat can be transferred for a given fin volume. Although optimization of individual fins has been investigated extensively (Krauss 1988; Aziz 1992) rarely has any effort been spent to optimize the design of integral plate fins. This is mainly because the temperature profile in an integral plate fin is essentially two-dimensional (2-D), and the temperature distribution cannot be obtained analytically.

Analysis of heat dissipation from the integral plate fin has been addressed in the past. Zabronsky (1955) determined the temperature distribution and efficiency of square fins around circular tubes in heat exchanger application. However, in his analysis, the adiabatic boundary condition at the fin edge has been satisfied exactly; whereas, the isothermal condition at the fin base has been satisfied only approximately.

On the other hand, Sparrow and Lin (1964) adopted a semi-analytical approach to solve the heat transfer equations in the fins and fin tube heat exchangers. Their analysis is applicable for both square and equilateral triangular arrays of tubes, which implies square and hexagonal circumferential fins around the fluid carrying tubes, respectively. Their solution has satisfied the isothermal boundary condition at the tube surface exactly. The adiabatic condition at the outer periphery of the fins has been satisfied approximately, but not to a desirable degree of accuracy. They observed the plate fin to be more efficient when the tubes are arranged in equilateral triangular arrays. They have further compared the performance of the square and hexagonal fins via-à-vis the performance of equivalent annular fins and found a marked derivation between efficiencies of polygonal fin and equivalent annular fin when (r_o^*/r_i) approaches unity.

Shah (1985) described an approximate method, referred to as "Sector Method," for determining the efficiency of plate fins. In this method, the fin is divided into a large number of small sectors. The approximate efficiency of each sector is determined from the efficiency curves already available for annular fins. Finally, the weighted average of the sector efficiencies gives the fin efficiency.

Kuan et al. (1984) numerically determined the efficiency of a variety of polygonal fins circumscribing tubes of different regular geometry. They found that for most combined tube and fin geometry, the efficiency can be calculated analytically, replacing the actual fin by an equivalent annular fin of the same surface area.

In the present paper, a method is described to find the dimensions of optimum plate fins that will maximize the heat dissipation for a given fin volume for different array arrangement of circular tubes. For the estimation of heat flux, the method of Sparrow and Lin (1964) is followed. The heat dissipation is expressed in terms of dimensional parameters of the fin geometry. Finally, the classical method of derivative is used to arrive at the optimum fin dimensions.

Analysis

In fin–tube heat exchangers, the tubes are most commonly arranged either in a square or in an equilateral triangular array, as shown in Figure 1. In such arrays, the heat from a particular

Address reprint requests to Dr. P. K. Das, Indian Institute of Technology, Department of Mechanical Engineering, Kharagpur 721302, India.

Received 26 July 1996; accepted 13 February 1997

Int. J. Heat and Fluid Flow 18: 530–537, 1997

655 Avenue of the Americas, New York, NY 10010

0142-727X/97/$17.00
PII S0142-727X(97)00029-5

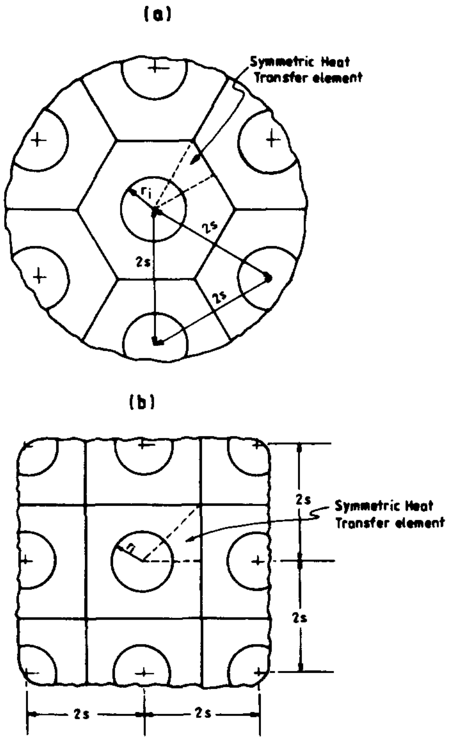

Figure 1 Tube arrangements in fin tube heat exchangers; (a) equilateral triangular array of tubes; (b) square array of tubes

tube is dissipated by a square or a hexagonal module of the plate circumscribing the tubes, respectively. In either case, a recurring section of the plate fin can be taken for the analysis of heat transfer. This section is basically a triangular sector with known isothermal condition at the fin base and adiabatic condition existing at the other boundaries. Figure 2 depicts the section of the fin, with ϕ_0 being $\pi/4$ and $\pi/6$, respectively, for square and equilateral triangular arrays of tubes. Considering a negligible temperature gradient normal to the fin surface for steady-state condition, the differential equation of heat transfer for the fin section can be written in nondimensional form as

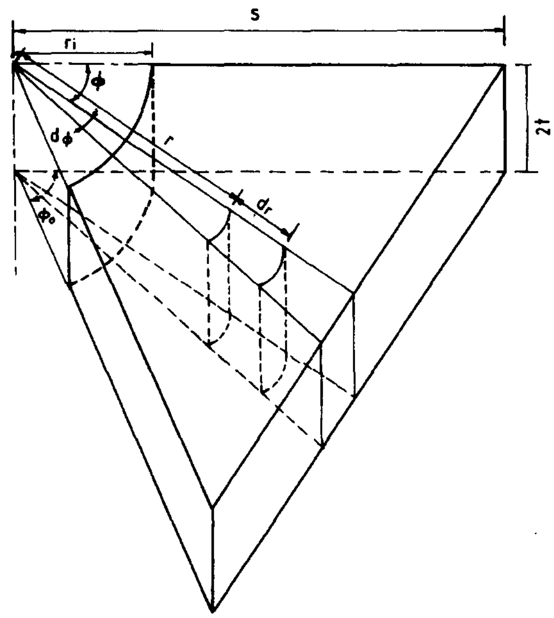

Figure 2 A symmetric section for heat transfer in plate fin

$$\frac{\partial}{\partial R}\left[R\frac{\partial\theta}{\partial R}\right]+\left[\frac{1}{R}\right]\frac{\partial^2\theta}{\partial\phi^2}=\left[\frac{\mathrm{Bi}}{T}\right]R\theta \tag{1}$$

Notation

- Bi — Biot number, based on fin base radius $[=(hr_i/k)]$
- C_n — constant
- h — heat transfer coefficient
- $I_n(Z)$ — modified Bessel function of first kind of order n and of argument Z
- j — discrete boundary point $(=1,2,3,\ldots,p)$
- k — thermal conductivity of fin material
- $K_n(Z)$ — modified Bessel function of second kind of order n and of argument Z
- n — an integer
- p — total number of discrete points
- Q — heat dissipation rate
- Q^* — dimensionless heat dissipation $\{=[Q/2kr_i\phi_0(T_w-T_a)]\}$
- Q_i — ideal heat dissipation rate
- Q_i^* — dimensionless ideal heat dissipation $\{=[Q_i/2kr_i\phi_0(T_w-T_a)]\}$
- Q_{opt} — optimum heat dissipation rate
- Q_{opt}^* — optimum dimensionless heat dissipation $\{=[Q_{opt}/2kr_i\phi_0(T_w-T_a)]\}$
- r — radial position of any point in the fin measured from the tube center
- r_i — radius of the tubes
- R — r/r_i
- r_o^* — outer radius of equivalent annular fins
- s — half-pitch length
- S — dimensionless half-pitch length $[=(s/r_i)]$
- t — half-fin thickness
- T — half-thickness of the fin in dimensionless form $[=(t/r_i)]$
- T' — fin temperature
- T_a — temperature of the surround gas medium of the fins
- t_{opt} — optimum half-thickness of the fins in dimensionless form
- T_{opt} — optimum dimensionless half-thickness of the fins in dimensionless form $[=(t_{opt}/r_i)]$
- T_w — fin base temperature
- V — fin volume
- V^* — dimensionless fin volume $[=(V/r_i^3)]$
- V_s — fin volume of triangular sector
- V_s^* — dimensionless fin volume of triangular sector $[=(V_s/r_i^3)]$
- Z_0 — parameter $(=\sqrt{\mathrm{Bi}/T})$
- Z_1 — parameter $[=(Z_0S/\cos\phi_j)]$

Greek

- θ — dimensionless temperature $[=(T'-T_a)/(T_w-T_a)]$
- λ — Eigen values or characteristics values $[=(n\pi/\phi_0)]$
- ϕ — angular position of any point in the fin
- ϕ_0 — angle of triangular sector is shown in Figure 2

The heat dissipation is assumed to be solely caused by convection. In an actual heat exchanger, radiative heat transfer also occurs. The radiative exchange is rather complex. It depends upon the size, arrangement, and spacing of the tubes, the distance between two successive fin plates, gas property, and surface and gas temperatures. However, in the case of low-temperature applications typical to fin–tube heat exchangers, analysis is done assuming convective dissipation only (Zukauskas 1981), because the radiative heat exchange is negligibly small.

Furthermore, the thermal conductivity of the fin material, the convective heat transfer coefficient, and the temperature of the surrounding fluid medium are taken as constants. The differential equation is subjected to the following nondimensional boundary conditions.

$$\text{at} \quad R=1 \quad \theta=1 \quad (0 \le \phi \le 0) \tag{2}$$

$$\text{at} \quad \phi=0 \quad \frac{\partial\theta}{\partial\phi}=0 \quad (1 \le R \le S) \tag{3}$$

$$\text{at} \quad \phi=\phi_0 \quad \frac{\partial\theta}{\partial\phi}=0 \quad \left(1 \le R \le \frac{S}{\cos\phi_0}\right) \tag{4}$$

$$\text{at} \quad 0 \le \phi \le \phi_0 \quad \frac{\partial\theta}{\partial N}=0 \quad \left(S \le R \le \frac{S}{\cos\phi_0}\right) \tag{5}$$

where N is normal to the boundary.

Following the analysis of Sparrow and Lin (1964), Equation 1 can be solve with boundary conditions 2 to 4 to get the temperature profile:

$$\theta(R,\phi) = \frac{I_0\left(R\sqrt{\frac{\mathrm{Bi}}{T}}\right)}{I_0\left(\sqrt{\frac{\mathrm{Bi}}{T}}\right)} + \sum_{n=0}^{p-1} C_n \cos\left(\frac{n\pi\phi}{\phi_0}\right) \cdot \left[\frac{K_\lambda\left(R\sqrt{\frac{\mathrm{Bi}}{T}}\right) I_\lambda\left(\sqrt{\frac{\mathrm{Bi}}{T}}\right) - K_\lambda\left(\sqrt{\frac{\mathrm{Bi}}{T}}\right) I_\lambda\left(R\sqrt{\frac{\mathrm{Bi}}{T}}\right)}{I_\lambda\left(\sqrt{\frac{\mathrm{Bi}}{T}}\right)}\right] \tag{6}$$

where C_n is a constant, and

$$\lambda = \frac{n\pi}{\phi_0} \tag{7}$$

Heat flow rate is given by

$$Q = -2tk\int_{\phi=0}^{\phi_0} (T_w - T_a)\left[\frac{\partial\theta}{\partial R}\right]_{R=1} \mathrm{d}\phi \tag{8}$$

$$\Rightarrow Q^* = \frac{\mathrm{Bi}}{Z_0}\left\{\frac{C_0[I_0(Z_0)K_1(Z_0)+K_0(Z_0)I_1(Z_0)] - I_1(Z_0)}{I_0(Z_0)}\right\} \tag{9}$$

where

$$Z_0 = \sqrt{\frac{\mathrm{Bi}}{T}} \tag{10}$$

Heat dissipation from the fin is, therefore, dependent on two parameters; namely, T and C_0. C_0 cannot be determined explicitly. Exploiting boundary condition (5), we get:

$$\sum_{n=0}^{p-1} C_n \cos\lambda\phi_j \left\{\frac{[K_\lambda(Z_1)I_\lambda(Z_0) - K_\lambda(Z_0)I_\lambda(Z_1)]}{I_\lambda(Z_0)}\right\} \cdot \left[\frac{\lambda(1+\tan\phi_j \tan\lambda\phi_j)}{Z_1} - \frac{I_\lambda(Z_0)K_{\lambda+1}(Z_1) + I_{\lambda+1}(Z_1)K_\lambda(Z_0)}{K_\lambda(Z_1)I_\lambda(Z_0) - K_\lambda(Z_0)I_\lambda(Z_1)}\right] = -\left[\frac{I_1(Z_1)}{I_0(Z_0)}\right] \tag{11}$$

where

$$Z_1 = \frac{Z_0 S}{\cos\phi_j} \tag{12}$$

For p discrete values of ϕ_j from 0 to ϕ_0, p linear equations are obtained from Equation 11. C_0 can be determined by solving these simultaneous equations. It should be noted at this point that C_0 is a sole function of the fin geometry and depends upon the choice of fin half-thickness T and half-pitch length S between the tubes.

Heat dissipation from an infinitely conducting fin can be determined readily,

$$Q_i^* = \frac{\mathrm{Bi}}{2\phi_0}(S^2\tan\phi_0 - \phi_0) \tag{13}$$

Therefore,
Fin efficiency:

$$\eta = \frac{Q^*}{Q_i^*} \tag{14}$$

Maximum heat dissipation for a given fin volume

From Equation 9, it can be seen that the rate of heat dissipation from the fin surface depends on C_0 and T. It has been shown further in the previous section that C_0 is a function of both T and S. However, for a constant fin volume, these two parameters are uniquely related:

$$V_s^* = T(S^2\tan\phi_0 - \phi_0) \tag{15}$$

and

$$V^* = \frac{2\pi}{\phi_0}V_s^* \tag{16}$$

Under the constraint of constant fin volume, only one of the two parameters of fin geometry can be varied independently. In the present exercise, half-thickness of the fin T has been taken as the independent variable. Therefore,

$$S = \sqrt{\frac{\phi_0(1+V^*/2\pi T)}{\tan\phi_0}} \tag{17}$$

Now S can be eliminated from Equation 12 using the above relationship, and ultimately, C_0 can be obtained from Equation 11 as a sole function of T for a constant fin volume V^*.

For maximum heat dissipation from the fin,

$$\frac{dQ^*}{dT} = \left\{ \frac{Z_0[I_0(Z_0)K_1(Z_0) + I_1(Z_0)K_0(Z_0)]}{I_0(Z_0)} \right\} \cdot \left\{ C_0 + \frac{C_0 Z_0}{2}\left[\frac{I_1(Z_0)}{I_0(Z_0)}\right] + T\frac{dC_0}{dT} \right\} + \frac{Z_0}{2}\left\{ Z_0 - 2\left[\frac{I_1(Z_0)}{I_0(Z_0)}\right] - Z_0\left[\frac{I_1(Z_0)}{I_0(Z_0)}\right]^2 \right\} = 0 \tag{18}$$

The above equation is a nonlinear, nonhomogeneous algebraic equation can can be solved by an iterative technique. It has been solved by the Newton–Raphson method as elaborated in the Appendix. The solution gives the unique value of the fin thickness for a given constant fin volume V^*. This optimum half-fin thickness can now be substituted in Equation 17. Carrying out the differentiation of Equation 18, we get

$$\frac{d^2Q^*}{dT^2} = \left\{ \left(\frac{Z_0^2}{4T}\right) \frac{[I_0(Z_0)K_1(Z_0) + I_1(Z_0)K_0(Z_0)]}{I_0(Z_0)} \cdot \left\{ 2C_0Z_0\left[\frac{I_1(Z_0)}{I_0(Z_0)}\right]^2 + 4T\left(\frac{C_0}{2T} + \frac{dC_0}{dT}\right)\left[\frac{I_1(Z_0)}{I_0(Z_0)}\right] - \left(C_0Z_0 + \frac{8T}{Z_0}\frac{dC_0}{dT} + \frac{4T^2}{Z_0}\frac{d^2C_0}{dT^2} \right) \right\} - \left[\frac{I_1(Z_0)}{I_0(Z_0)}\right] \left\{ 2Z_0\left[\frac{I_1(Z_0)}{I_0(Z_0)}\right]^2 + (Z_0+1)\left[\frac{I_1(Z_0)}{I_0(Z_0)}\right] - \left(2Z_0 + 2 - \frac{2}{Z_0} \right) \right\} - \left(\frac{3Z_0}{2} - 2 \right) \tag{20}$$

It has been confirmed that the expression above has a negative value for the optimum value of T obtained from Equation 18.

Results and discussion

Equation 18 has been solved numerically for different fin volumes and Biot numbers. Fin geometry for both square and triangular arrays of tubes have been considered. Results are summarised below.

Heat dissipation from hexagonal fins as a function of plate thickness is depicted in Figure 3a and b for typical parametric ranges. For a fixed fin volume, heat dissipation increases with plate thickness, reaches a well-defined maximum, and then falls gradually. It can be noted further that, although the heat dissipation is insensitive to fin volume at lower values of plate thickness, there is an optimum plate thickness that maximizes the heat dissipation for a particular fin volume. Moreover, the optimum plate thickness increases with the fin volume.

The influence of Biot number on the performance of hexagonal fins can also be understood by comparing Figure 3a and b. Although, with the increase of Biot number, the nature of the curves remain the same, the optimum plate thickness increases

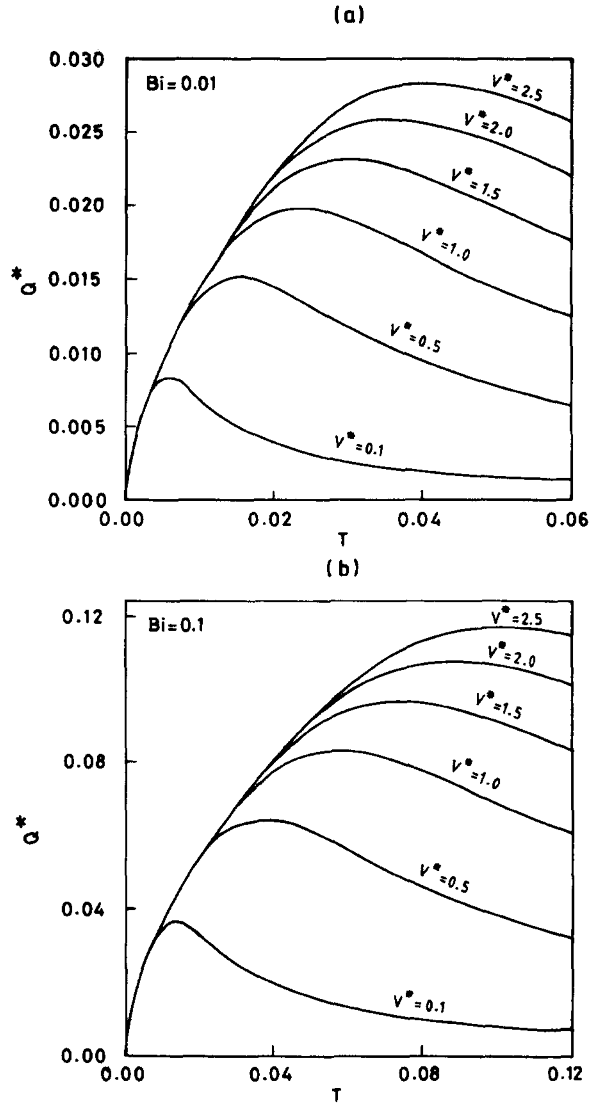

Figure 3 Variation of heat dissipation with fin thickness for hexagonal array of tubes

for a particular fin volume. This increase in the optimum plate thickness is also associated with increased heat dissipation.

As with hexagonal fins, maximum heat dissipation in the case of square fins occurs for a well-defined optimum plate thickness for a given fin volume. This is graphically represented in Figure 4a and b. From these two figures, it can also be noted that an increase of Biot number has the same effect on the optimum dimension of the square fins as has been observed in the case of hexagonal fins.

In the present analysis, the optimum fin thickness has been determined from Equation 18 for a fixed fin volume. The existence of optimum fin dimensions for a given fin volume can be demonstrated alternatively by studying the variation of heat dissipation with the half-pitch length S. In this case, the derivative of heat dissipation given in Equation 9 has to be taken with respect to S, and an equation similar to Equation 18 will be obtained. This is not shown here, but the results are presented in Figure 5a and b for square and hexagonal fins, respectively, for a Biot number of 0.1. In the figure, the loci of the optimum half-pitch lengths for different fin volumes is shown by dotted lines. Comparing Figure 5a with Figure 4b and figure 5b with Figure 3b, it can be seen that, for a particular fin volume, the

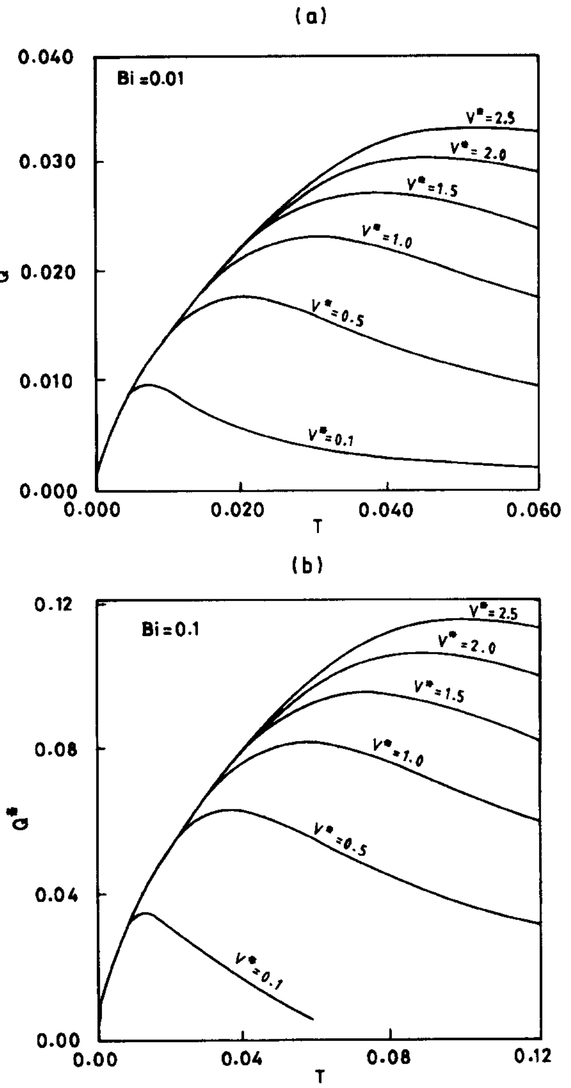

Figure 4 Variation of heat dissipation with fin thickness, for square array of tubes

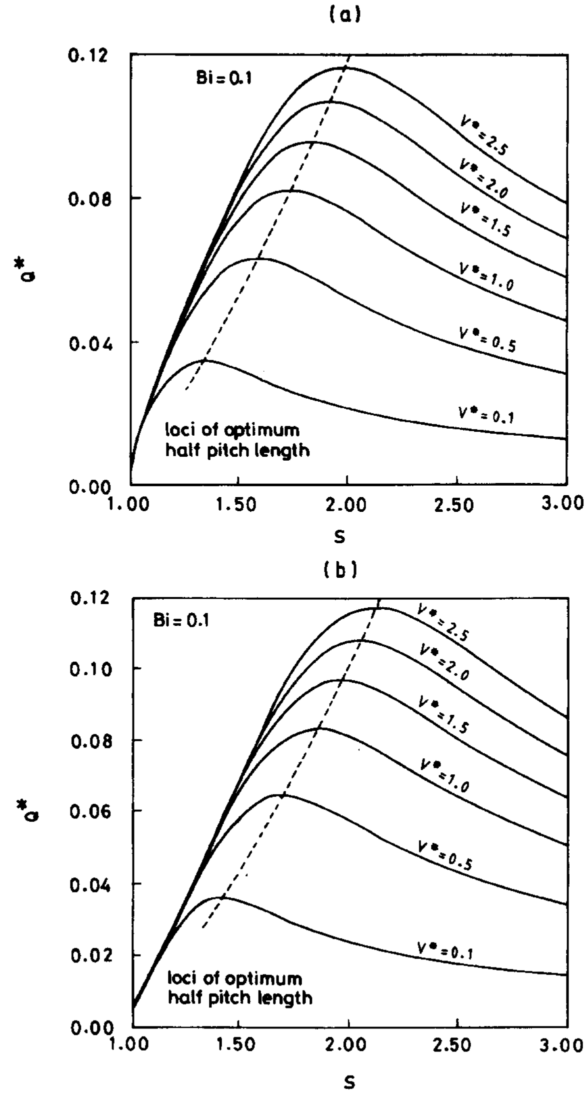

Figure 5 Variation of heat dissipation with pitch length; (a) square array of tubes; (b) Hexagonal array of tubes

optimum pitch length is related to the optimum fin thickness through Equation 17.

Next, plots have been generated for arriving at the optimum design of integral fin tube assembly for both in-line and staggered arrangements of tubes. The families of curves presented in Figure 6 can be used as a guide for designing square fins. Once the required heat duty for a square fin is fixed, the Biot number must be determined. For this, h should be estimated from the prevailing convective conditions, and k and r_i should be available. Known values of heat dissipation and Biot number fix the design point of the desirable fin on the plane of Figure 6. From the design point, both the optimum fin thickness and corresponding fin volume can be obtained directly. From these two pieces of information, the optimum pitch length and fin efficiency can be calculated using Equations 17 and 14, respectively. Similar design plots for hexagonal fins are provided in Figure 7.

For many years, it was common design practice to replace the polygonal fin of a plate fin heat exchanger by an equivalent annular fin (Threlkeld 1970) of the same volume. By this simplification, an approximate, but analytical, expression of fin efficiency can be obtained. Sparrow and Lin (1964) reported parametric ranges where there is a large deviation between the performance

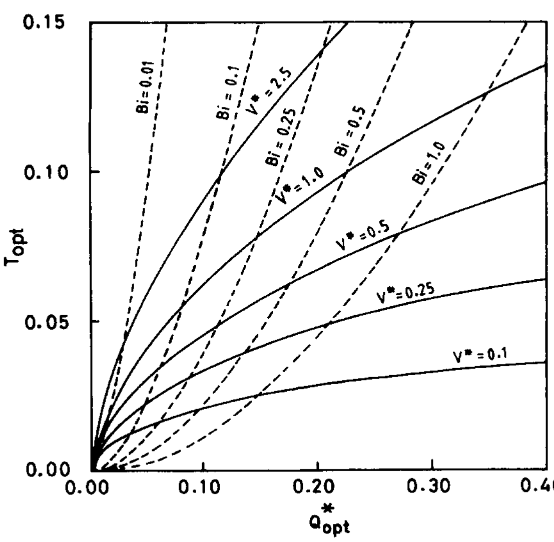

Figure 6 Design curves for optimum plate fins for square array of tubes

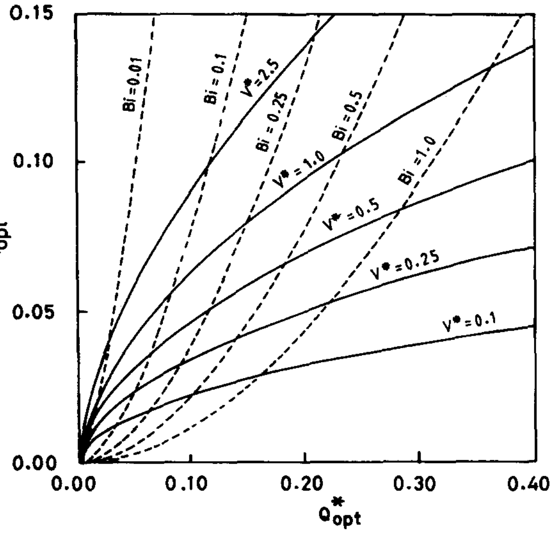

Figure 7 Design curves for optimum plate fins for equilateral triangular array of tubes

of the equivalent annular fin and the actual plate fin. They also noted this deviation to be greater in the case of the square fins, as compared to hexagonal fins. Kaun et al. (1984) observed that the concept of equivalent annular fin yields accurate results for most of the combination of tubes and fins of regular shape, except for the case of very elongated symmetric elements. In the present work, an effort was made to verify whether the concept of equivalent fin can be extended to calculate the optimum fin dimensions.

By definition, an equivalent annular fin has the same volume as the actual fin. Conventionally, because the thicknesses of both the fins are taken to be identical, an equivalent fin has the same surface area as the actual fin. However, in the present case, although the constancy of volume between the actual and equivalent fin has been maintained, their thicknesses have not been take to be the same. For a particular fin volume, optimum dimensions for the actual fin and the annular fin have been determined.

Brown (1965) has expressed the total heat dissipation from the annular fin as a function of the thickness and the volume of the fin. Optimum thickness for the annular fin has been obtained using Equation (3) of Brown, applying the classical derivative

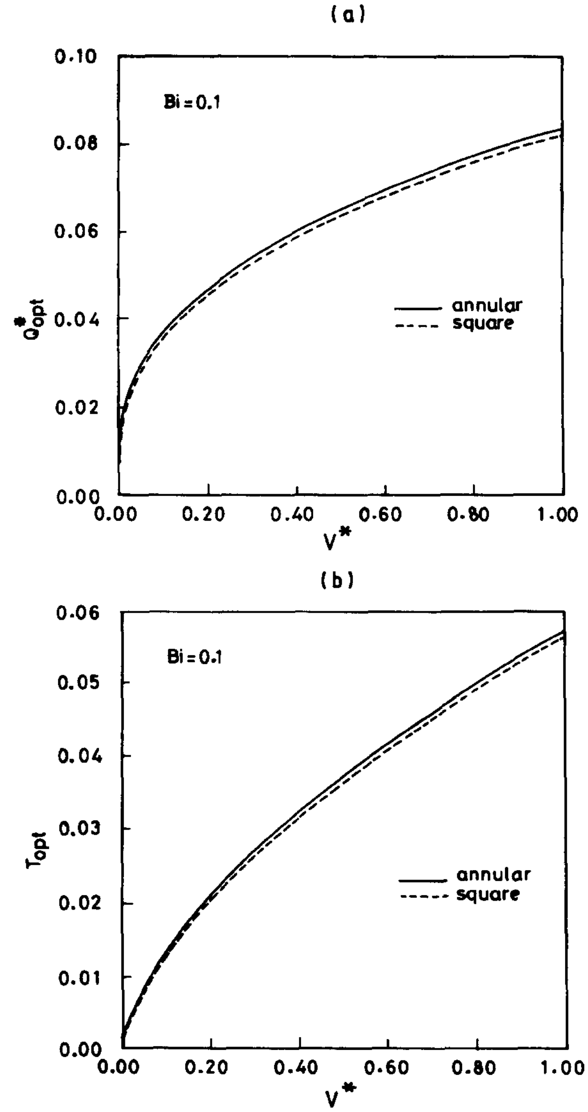

Figure 8 Comparison between optimum square and annular fins of same volume; (a) variation of maximum heat dissipation with volume; (b) variation of optimum thickness with volume

Table 1 Comparison of different optimum fins of identical volume for Bi=0.1

V^*	Square fin			Hexagonal fin			Annular fin		
	T_{opt}	Q^*_{opt}	η	T_{opt}	Q^*_{opt}	η	T_{opt}	Q^*_{opt}	η
0.1	0.0127	0.0351	0.5605	0.01323	0.0363	0.6031	0.0133	0.0365	0.6102
0.3	0.0261	0.0526	0.5759	0.02672	0.0538	0.6016	0.0268	0.0539	0.6053
0.5	0.0363	0.0636	0.5798	0.03690	0.0647	0.6000	0.0370	0.0648	0.6027
0.7	0.0450	0.0720	0.5815	0.04560	0.0731	0.5987	0.0457	0.0733	0.6010
0.9	0.0527	0.0791	0.5824	0.05337	0.0802	0.5977	0.0534	0.0804	0.5996
1.0	0.0564	0.0822	0.5827	0.05700	0.0834	0.5972	0.0571	0.0835	0.5991
1.2	0.0632	0.0880	0.5830	0.06386	0.0892	0.5964	0.0634	0.0893	0.5981
1.4	0.0697	0.0932	0.5832	0.07029	0.0944	0.5956	0.0704	0.0946	0.5972
1.5	0.0728	0.0957	0.5833	0.07336	0.0969	0.5953	0.0734	0.0970	0.5968
1.8	0.0815	0.1025	0.5836	0.08215	0.1036	0.5944	0.0822	0.1038	0.5958
2.0	0.0871	0.1066	0.5834	0.08768	0.1078	0.5939	0.0877	0.1080	0.5952
2.2	0.0924	0.1105	0.5833	0.09299	0.1117	0.5934	0.0931	0.1118	0.5941
2.5	0.0999	0.1161	0.5832	0.10063	0.1172	0.5927	0.1007	0.1173	0.5939

technique, as has been done for the plate fins in the present work under the constraint of constant volume. Results of this exercise for the square fin and equivalent annular fin are shown in Figure 8a and b for a Biot number of 0.1. From Figure 8a, it can be seen that an optimum annular fin dissipates more heat than the optimum square fin for the same fin volume, although the difference in the rate of heat dissipation is only marginal. Figure 8b compares the optimum thickness of square and equivalent annular fins. From the last two figures, it is evident that optimum square fins can be designed taking the dimensions of equivalent annular fins without much loss of accuracy. It has been verified further that the performance of the optimum square fin can be approximated by that of an equivalent annular fin, even for other Biot numbers.

A similar exercise of comparison between an optimum hexagonal fin and equivalent annular fin have begun. From the results of Table 1, it can be seen that the dimensions and performance of actual hexagonal fins are better approximated by equivalent annular fins compared to square fins.

Conclusion

In this study, a method was developed to determine the optimum dimension of the plate fins of a fin tube heat exchanger. Two common arrangements of tubes; namely, square and equilateral triangular arrays, were considered. However, this method can be employed for other arrays of tubes and also for individual polygonal fins circumscribing a circular tube.

It can be seen that, even under the optimum design condition, more heat is dissipated by the fin surface for a fixed fin volume when the tubes are arranged in an equilateral triangular array. Finally, it was demonstrated that optimum fin dimension can be calculated from the concept of equivalent annular fin sacrificing little accuracy.

References

Aziz, A. 1992. Optimum dimensions of extended surfaces operating in a convective environment. *Appl. Mech. Rev.*, **45**, 155–173

Brown, A. 1965. Optimum dimensions of uniform annular fins. *Int. J. Heat Mass Transfer*, **8**, 655–662

Kraus, A. D. 1988. Sixty-five years of extended surface technology (1922–1987). *Appl. Mech. Rev.*, **11**, 321–364.

Kuan, D. Y., Aris, R. and Davis, H. T. 1984. Estimation of fin efficiencies of regular tubes arrayed in circumferential fins. *Int. J. Heat Mass Transfer*, **22**, 148–151

Shah, R. K. 1985. Compact Heat Exchangers. In *Handbook of Heat Transfer Applications*, 2nd ed., W. M. Rohsenow, J. P. Hartnett, and E. N. Ganic (eds.). McGraw-Hill, New York, 4-174–4-311

Sparrow, E. M. and Lin, S. H. 1964. Heat transfer characteristics of polygonal and plate fins. *Int. J. Heat Mass Transfer*, **7**, 951–953.

Threlkeld, J. L. 1970. *Thermal Environmental Engineering*, 2nd ed. Prentice-Hall, Englewood Cliffs, NJ, 245

Zabronsky, H. 1955. Temperature distribution and efficiency of a heat exchanger using square fins on round tubes. *J. Appl. Mech.*, **22**, 119–122

Zukauskas, A. 1981. Air-cooled heat exchangers. Heat exchangers thermal-hydraulic fundamentals and design. Kakac, S., Bergles, A. E. and Mayinger, F. (eds.). *Hemisphere*, Bristol, PA, 49–83

Appendix

The Newton–Raphson technique is applied to determine the optimum value of plate thickness from Equation 18. The plate thickness is obtained from the following general expression

$$T_{m+1} = T_m - \frac{f(T_m)}{f'(T_m)} \tag{A1}$$

where the subscripts denote the value at a particular iteration. From Equation 18

$$\begin{aligned} f(T) = &\left\{\frac{Z_0}{I_0(Z_0)}[I_0(Z_0)K_1(Z_0)+I_1(Z_0)K_0(Z_0)]\right\} \\ &\cdot\left\{C_0 + \frac{C_0 Z_0}{2}\left[\frac{I_1(Z_0)}{I_0(Z_0)}\right] + T\frac{\mathrm{d}C_0}{\mathrm{d}T}\right\} \\ &+ \frac{Z_0}{2}\left\{Z_0 - 2\left[\frac{I_1(Z_0)}{I_0(Z_0)}\right] - Z_0\left[\frac{I_1(Z_0)}{I_0(Z_0)}\right]^2\right\} \end{aligned} \tag{A2}$$

and

$$\begin{aligned} f'(T) = &\left\{\left(\frac{Z_0^2}{4T}\right)\frac{[I_0(Z_0)K_1(Z_0)+I_1(Z_0)K_0(Z_0)]}{I_0(Z_0)}\right\} \\ &\cdot\left\{2C_0Z_0\left[\frac{I_1(Z_0)}{I_0(Z_0)}\right]^2 + 4T\left(\frac{C_0}{2T}+\frac{\mathrm{d}C_0}{\mathrm{d}T}\right)\left[\frac{I_1(Z_0)}{I_0(Z_0)}\right]\right. \\ &\left.+\left(C_0Z_0 + \frac{8T}{Z_0}\frac{\mathrm{d}C_0}{\mathrm{d}T} + \frac{4T^2}{Z_0}\frac{\mathrm{d}^2C_0}{\mathrm{d}T^2}\right)\right\} \\ &-\left[\frac{I_1(Z_0)}{I_0(Z_0)}\right]\left\{2Z_0\left[\frac{I_1(Z_0)}{I_0(Z_0)}\right]^2\right. \\ &\left.+(Z_0+1)\left[\frac{I_1(Z_0)}{I_0(Z_0)}\right] - \left(2Z_0 + 2 - \frac{2}{Z_0}\right)\right\} \\ &-\left(\frac{3Z_0}{2} - 2\right) \end{aligned} \tag{A3}$$

Knowing the values of C_0 and $(\mathrm{d}C_0/\mathrm{d}T)$, $f(T)$ can be evaluated. C_0 can be determined for known values of V^* and an estimated value of T from Equation 11, as explained earlier. Next, Equation 11, must be differentiated with respect to T, which gives

$$\begin{aligned} \sum_{n=0}^{p-1} C_n &\left\{\left[\frac{\lambda\cos\lambda\phi_j(1+\tan\phi_j\tan\lambda\phi_j)}{Z_1}\right]\right. \\ &\left.\cdot\left[\frac{I_\lambda(Z_0)K_\lambda(Z_1) - I_\lambda(Z_1)K_\lambda(Z_0)}{I_\lambda(Z_0)}\right]\right\} \\ &\cdot\left\{\left[\frac{2T}{Z_0C_n}\frac{\mathrm{d}C_n}{\mathrm{d}T}\right.\right. \\ &\left.+\frac{Z_0(2V^* + T\phi_0)(1-\lambda)}{TZ_1^2\tan\phi_0\cos^2\phi_j} + \frac{I_{\lambda+1}(Z_0)}{I_\lambda(Z_0)}\right] \\ &-\left[\frac{I_{\lambda+1}(Z_0)K_\lambda(Z_1) + I_\lambda(Z_1)K_{\lambda+1}(Z_0)}{I_\lambda(Z_0)K_\lambda(Z_1) - I_\lambda(Z_1)K_\lambda(Z_0)}\right] \end{aligned}$$

$$+\frac{Z_0(2V^*+T\phi_0)}{TZ_1\tan\phi_0\cos^2\phi_j}$$

$$\cdot\left[\frac{I_\lambda(Z_0)K_{\lambda+1}(Z_1)+I_{\lambda+1}(Z_1)K_\lambda(Z_0)}{I_\lambda(Z_0)K_\lambda(Z_1)-I_\lambda(Z_1)K_\lambda(Z_0)}\right]\Bigg\}$$

$$-\sum_{n=0}^{p-1}C_n\Bigg\{\cos\lambda_j$$

$$\cdot\left[\frac{I_\lambda(Z_0)K_{\lambda+1}(Z_1)+I_{\lambda+1}(Z_1)K_\lambda(Z_0)}{I_\lambda(Z_0)}\right]\Bigg\}$$

$$\cdot\Bigg\{\left[\frac{2T}{Z_0C_n}\frac{\mathrm{d}C_n}{\mathrm{d}T}+\frac{I_{\lambda+1}(Z_0)}{I_\lambda(Z_0)}+\frac{Z_0(2V^*+T\phi_0)(1+\lambda)}{TZ_1^2\tan\phi_0\cos^2\phi_j}\right]$$

$$+\frac{Z_0(2V^*+T\phi_0)}{TZ_1\tan\phi_0\cos^2\phi_j}$$

$$\cdot\left[\frac{I_\lambda(Z_0)K_\lambda(Z_1)-I_\lambda(Z_1)K_\lambda(Z_0)}{I_\lambda(Z_0)K_{\kappa+1}(Z_1)+I_{\lambda+1}(Z_1)K_\lambda(Z_0)}\right]$$

$$+\left[\frac{I_{\lambda+1}(Z_1)K_{\lambda+1}(Z_0)-I_{\lambda+1}(Z_0)K_{\lambda+1}(Z_1)}{I_\lambda(Z_0)K_{\lambda+1}(Z_1)+I_{\lambda+1}(Z_1)K_\lambda(Z_0)}\right]\Bigg\}$$

$$=\frac{Z_0(2V^*+T\phi_0)}{TZ_1\tan\phi_0\cos^2\phi_j}\left[\frac{I_0(Z_1)}{I_0(Z_0)}-\frac{I_1(Z_1)}{Z_1I_0(Z_0)}\right]$$

$$-\left[\frac{I_1(Z_1)I_1(Z_0)}{I_0(Z_0)I_0(Z_0)}\right] \tag{A4}$$

This system of p equations contains C_n and $(\mathrm{d}C_n/\mathrm{d}T)$, where $n=0,1,2,3,\ldots,p-1$, with known values of C_n. Therefore, $(\mathrm{d}C_n/\mathrm{d}T)$, hence $(\mathrm{d}C_0/\mathrm{d}T)$ can be determined.

The expression of $f'(T)$ contains $(\mathrm{d}^2C_0/\mathrm{d}T^2)$ in addition to C_0 and $(\mathrm{d}C_0/\mathrm{d}T)$. For determining $(\mathrm{d}^2C_0/\mathrm{d}T^2)$ Equation A4 must be differentiated, and the methods described above must be repeated.